SYNTHETIC STRATIGRAPHY WITH A STOCHASTIC DIFFUSION MODEL OF FLUVIAL SEDIMENTATION

JON D. PELLETIER AND DONALD L. TURCOTTE

Snee Hall, Cornell University, Ithaca, New York 14853, U.S.A.

ABSTRACT: Models of stratigraphic completeness and bed formation in fluvial depositional environments have most often assumed that successive depositional and erosional events deposit or erode amounts of sediment independently. This results in a random-walk model for the total amount of deposited sediment locally as a function of time. We consider an extension of the random-walk model of sedimentation in an alluvial plain in which deposition or erosion is concentrated in randomly avulsing channels and sediment transport is modeled by the diffusion equation (Culling's model). In contrast to the random-walk model, this model results in an anticorrelated sequence locally as a function of time, i.e., after an area has aggraded it has a higher elevation and a lower rate of future aggradation. In a previous paper we analyzed the topography generated by the model and argued that porosity variations could be associated with topographic variations. The power spectrum S (the square of the coefficients in a Fourier series) of one-dimensional transects of topography and porosity horizontally and vertically in this model have a power-law dependence on wave number k: $S(k) \propto k^{-\beta}$, with values of β close to those observed. In this paper we show that the model deposits sediment with a rate depending on time interval as a power law with exponent $-\frac{3}{4}$, more consistent with observations than the random-walk model. The model produces an exponential bed-thickness distribution with a skew dependent on the sedimentation rate of the basin in accordance with observations. We also examine the persistence in the series of bed thicknesses as a function of depth. For the stochastic diffusion model of sedimentation no persistence is observed. If the model fully characterizes the autocyclic dynamics in fluvial sedimentary basins, the lack of persistence in the synthetic bed sequences suggests that observed persistence and cyclicity in real bed-thickness sequences must be the result of allocyclic processes.

INTRODUCTION

Variations in density and porosity in a sedimentary basin along a one-dimensional horizontal or vertical transect can be analyzed with techniques from time series analysis. Variations in density or porosity can be characterized with the probability density function and the power spectrum. The probability density function or distribution quantifies how the data is distributed about the mean. Two examples of probability density functions are the normal and lognormal distributions. The power spectrum S measures the persistence of the data. The power spectrum is defined as the square of the coefficients in a Fourier series representation of the transect. It measures the average variation of the function at different wavelengths. If adjacent data points are totally uncorrelated then the power spectrum is constant as a function of wave number (the reciprocal of the wavelength), i.e., white noise. If adjacent values are strongly correlated relative to points far apart, the power spectrum is large at small wave numbers (long wavelengths) and small at large wave numbers (short wavelengths).

In the past decade many studies have documented the scale invariance of porosity and density variations in sedimentary basins. Scale invariance means that the power spectrum S of porosity and density vertically and horizontally in sedimentary basins has a power-law dependence on wave number k: $S(k) \propto k^{-\beta}$. Power-law power spectra of vertical density and porosity well logs have been reported by Hewett (1986), Walden and Hosken (1985), Pilkington and Todoeschuck (1990), Todoeschuck et al. (1990), Holliger (1996), and Pelletier and Turcotte (1996). Tubman and Crane (1995) have presented evidence for scale-invariant horizontal variations in

density and porosity from well logs and seismic data. In addition, Dunne et al. (1995) presented evidence that the topography of alluvial plains perpendicular to the channel dip is also scale invariant. They performed spectral analysis of transects of fluvial microtopography of an alluvial plain in Kenya, and they obtained power spectra roughly consistent with $S(k) \propto k^{-2}$.

A related problem to the statistics of topography and porosity variations in sedimentary basins is the statistics of preserved sections. Stratigraphic sections are formed by alternating periods of deposition and erosion or nondeposition. The resulting stratigraphic section contains the deposited sediments that have not been subsequently eroded. Various stochastic models have been proposed to explain aspects of sedimentary bed formation, including the frequency distribution of bed thicknesses. Beginning with Kolmogorov's work (Kolmogorov 1951), many studies have investigated random-walk models of sedimentation. As mentioned above, random-walk models assume that the magnitudes of alternating depositional and erosional events are independent. These models are applied by letting the typical episodes of deposition and erosion define minimal units of a discrete time scale. The lengthy periods of nondeposition, as well as any long intervals of deposition and erosion, are treated as multiples of these units. There have been a number of variants of Kolmogorov's work: Schwarzacher (1975) described a process of bed formation that results in a random walk on the integers, Dacey (1979) considered both exponential and geometrical probability distributions for the amount of sediment deposited and eroded, and Strauss and Sadler (1989) have considered a continuous version of the random-walk model. These models are generally considered to be successful at predicting observed bed-thickness distributions (Strauss and Sadler 1989).

Tipper (1983) was the first to apply the random-walk model to the problem of stratigraphic completeness: given that deposited sediment is often later eroded, how much of the depositional history is preserved in a given stratigraphic section? Sadler (1981) obtained a solution to this problem by investigating the dependence of sedimentation rate on the time span over which the sedimentation rate was measured. If the dependence of the sedimentation rate on time span can be assessed, then for a single stratigraphic section, the ratio of the overall accumulation rate to the average rate at time span T is the completeness (Sadler and Strauss 1990). Sadler quantified the sedimentation rate, R, as a power-law function of time span, T, with exponent -0.65: $R \propto T^{-0.65}$. Sadler interpreted the decreasing sedimentation rate with time as the result of including longer and longer hiatuses of erosion or nondeposition in the average at longer time intervals. Plotnick (1986) introduced a fractal model for the length distribution of stratigraphic hiatuses that is consistent with this interpretation and predicts a power-law dependence of sedimentation rate on time span. Tipper (1983), Strauss and Sadler (1989), and Sadler and Strauss (1990) have addressed the issue of stratigraphic completeness with the random-walk model of sedimentation. The random-walk model predicts a power-law dependence of sedimentation rate on time with exponent $-\frac{1}{2}$: $R \propto T^{-\frac{1}{2}}$, giving quite good agreement with Sadler's data.

The observation of scale invariance in topography and porosity variations in sedimentary basins motivated Pelletier and Turcotte (1996) to present a model for the topography of an alluvial plain evolving by deposition and erosion that exhibits scale invariance in space and time. In their model, deposition and erosion were concentrated in channels that avulsed randomly in space and time across the alluvial plain. Channel avulsion has most often been modeled as a stochastic process because of its complexity and

unpredictability (Bridge and Leeder 1979; Mackey and Bridge 1995). In the model of Pelletier and Turcotte (1996) sediment transport was governed by the diffusion equation. Although the mechanics of sediment transport are complex, a simple diffusion model has been successfully applied to the profile of sediment thickness and grain size perpendicular to the channel direction (Pizzuto 1987; Guccione 1993). There is abundant evidence for the applicability of the diffusion equation to model topography resulting from sediment transport processes. Culling (1965) hypothesized that the horizontal flux of eroded material on a hillslope was proportional to the slope. With conservation of mass this yields the diffusion equation. Begin et al. (1981) have derived the diffusion equation for the evolution of channel profiles using assumptions similar to those of Culling (1965), but beginning with classic equations of sediment transport. Solutions to the diffusion equation have been applied successfully to model alluvial fans, prograding deltas, eroding fault scarps, and the longitudinal profiles of laboratory channels (Wallace 1977; Nash 1980; Begin et al. 1981; Gill 1983a, 1983b; Hanks et al. 1984; Hanks and Wallace 1985; Kenyon and Turcotte 1985). Pelletier and Turcotte (1996) did not consider allocyclic processes such as tectonic or climatic forcing in their model.

In the simplest version of their model, Pelletier and Turcotte (1996) assumed that channels were parallel and of uniform capacity along the direction of the channels. This reduced the model to two spatial dimensions: the height h of the topographic profile and the direction x perpendicular to the direction of the channels. The model equation they studied is

$$\frac{\partial h(x,\, t)}{\partial t} = D\frac{\partial^2 h(x,\, t)}{\partial x^2} + \eta(x,\, t) \tag{1}$$

where D is the diffusion coefficient and $\eta\,(x,\, t)$ is a Gaussian, white noise. This equation is known as the Edwards–Wilkinson equation in the physics literature on stochastic surface growth (Edwards and Wilkinson 1982).

The term $\eta\,(x,\, t)$ represents actual deposition and erosion. The assumed Gaussian white noise is characterized by a mean, $\bar{\eta}$, and a standard deviation σ. If $\bar{\eta} = 0$ there is no net change in elevation of the basin: deposition balances erosion. For $\bar{\eta} > 0$ there is net deposition and for $\bar{\eta} < 0$ there is net erosion. The ratio $\sigma/\bar{\eta}$ is a measure of the amplitude of fluctuations in the sedimentation process.

The spectral behavior of the topography resulting from Eq 1 in both space and time can be obtained with Laplace transform techniques. Pelletier and Turcotte (1996) found that the power spectrum of the surface generated by Eq 1 is $S(k) \propto k^{-2}$, in agreement with the power spectral analyses of the topography of the Kenyan alluvial plain by Dunne et al. (1995). The power spectrum of variations in the elevation of a position on the surface relative to the mean elevation in time is given by $S(f) \propto f^{-3/2}$. If deposition and erosion took place independently, the variation of the local elevation relative to the mean with time would be a random walk with power spectrum $S(f) \propto f^{-2}$. The effect of the diffusion term is to preferentially fill low-lying areas of the alluvial plain. This results in an anticorrelated sequence of deposition and erosion: after an area has aggraded it has a higher elevation and a lower rate of future aggradation. Without the presence of the diffusion term, the surface would be white noise. In Figure 1, we present examples of (a) Gaussian white noise, (b) a Gaussian time series with $S(k) \propto k^{-2}$ (a Brownian walk), and (c) one of the topographic transects of Dunne et al. (1995). It is clear from the statistical similarity of Figures 1B and 1C that the presence of the diffusion term results in a more realistic topography than the white noise of Figure 1A.

As Pelletier and Turcotte (1996) show, the power spectra of spatial and temporal variations in the model topography are unchanged when the assumption of parallel channels is relaxed to include any angular probability distribution of channel directions. In addition, they argued that since grain-size variations are coupled to the topographic profile perpendicular to the channel direction with the coarsest material deposited in topographic depressions such as channel-fill deposits, porosity variations may exhibit the
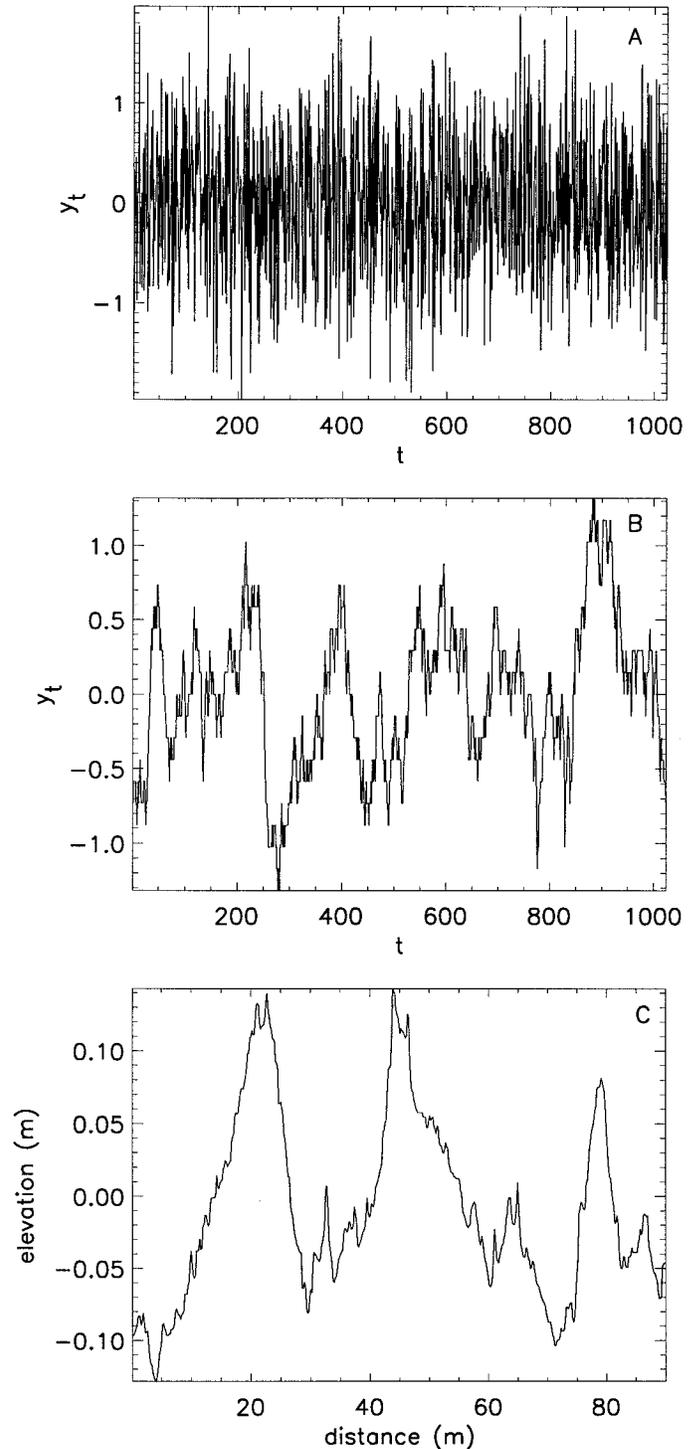

FIG. 1.—Examples of **A)** white noise ($S(k)$=constant) and **B)** a Brownian walk. **C)** One-dimensional transect of hillslope topography perpendicular to the channel dip obtained with laser altimetry (from Dunne et al. 1995).

same power spectral dependence as the topographic profile. This hypothesis implies that the vertical porosity variations should have the same power spectral exponent, $-3/2$, as the variations in local elevation in time. Pelletier and Turcotte (1996) presented power spectra of vertical porosity well logs from fifteen wells in the Gulf of Mexico with an average power spectral exponent of -1.4, lending support to their hypothesis. Similarly, Dolan

et al. (unpublished work) obtained average power spectral exponents −1.50, −1.62, and −1.46 using three different numerical procedures for a cluster of ten wells in a fluvial sedimentary environment.

Although random-walk models of sedimentation reproduce the observed dependence of sedimentation rate on time, they are unrealistic in that they do not allow sediment to be transported laterally on the alluvial plain. If sediment is deposited on an alluvial plain and there is no lateral transport, the topography of the alluvial plain is completely uncorrelated above the length scale of the size of depositional units. An example of the uncorrelated topography produced by the random-walk model is illustrated in Figure 1A. Clearly a very unrealistic topography results from the random-walk model. A goal of this paper is to determine the effect of diffusive sediment transport on the quantitative analysis of stratigraphic completeness and the distribution and persistence of bed thicknesses. We will compare the predictions of the synthetic stratigraphies of the model equation (Eq 1) with the random-walk model and with observations.

The presence of cyclic behavior in stratigraphic sequences has been an active area of research for many years (Beerbower 1964; DeBoer and Smith 1994). We will investigate the persistence of bed-thickness sequences produced by the stochastic diffusion model with and without periodic forcing in order to ascertain the likelihood that persistence and cyclicity in bed-thickness sequences are due to autocyclic (internal) or allocyclic (external) processes.

SEDIMENTATION RATE VS. TIME

The time history of sedimentation with constant rate of subsidence based on our model is given in Figure 2. Figure 2A is the complete history of deposition and erosion in the basin. The time series of deposition and erosion is represented by a Gaussian time series with power spectrum $S(f) \propto f^{-3/2}$, representing the elevation or total height of sediment deposited locally in a fluvial sedimentary basin, superimposed on a constant rate of subsidence.

The time series was synthesized with the Fourier filtering method (Turcotte 1992). This technique proceeds in several steps:

(1) We consider 2^N incremental steps of length ΔT. Each step is given a random value d_n based on the Gaussian probability distribution. This is a Gaussian noise sequence. Adjacent values are totally uncorrelated.

(2) A discrete Fourier transform is taken of the random values. The Fourier coefficients are given by

$$D_m = \Delta T \sum_{n=0}^{N-1} d_n e^{2\pi inm/N} \qquad (2)$$

This transform maps N real numbers (the d_n) into N complex numbers (the D_m). Because the transform is taken of a Gaussian white noise sequence the Fourier transform is flat. Except for the statistical scatter the amplitudes of the D_m are equal.

(3) The resulting Fourier coefficients D_m are filtered using the relation

$$D'_m = \left(\frac{m}{N-1}\right)^{\beta/2} D_m \qquad (3)$$

The power $\beta/2$ is used because the power spectral density is proportional to the amplitude squared. The amplitudes of the small-m coefficients correspond to short wavelengths λ_m and large wave numbers $k_m = 2\pi/\lambda_m$. The large-m coefficients correspond to long wavelengths and small wave numbers.

(4) An inverse discrete Fourier transform is taken of the filtered Fourier coefficients. The sequence of points is given by

$$d'_n = \frac{1}{N\Delta T} \sum_{m=0}^{N-1} D'_m e^{-2\pi inm/N} \qquad (4)$$

A time series synthesized in this way is superimposed on a linear trend
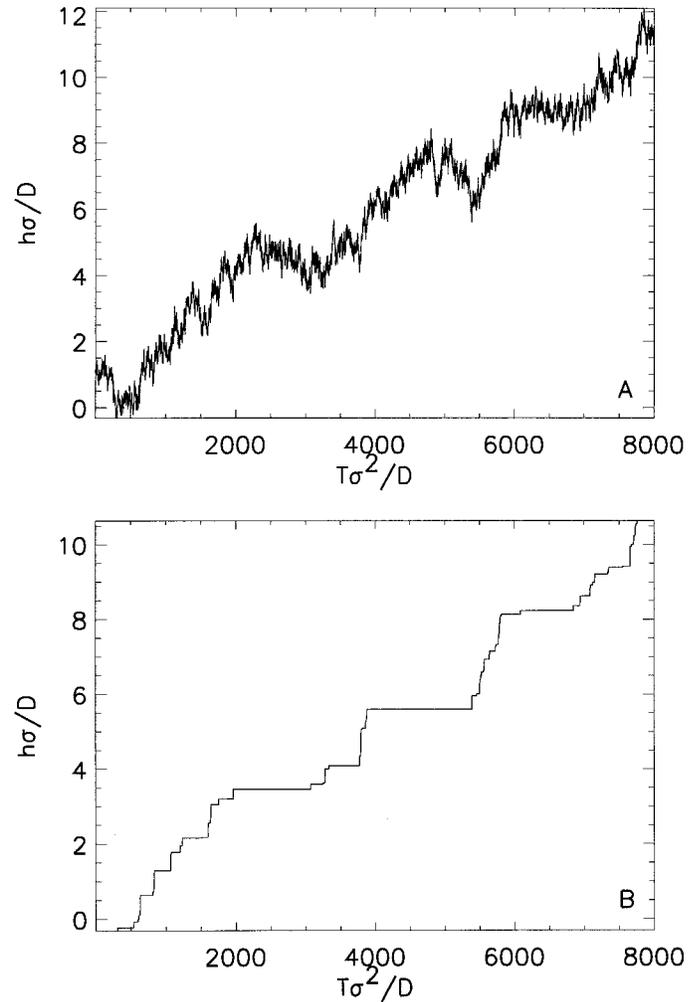

FIG. 2.—**A)** The nondimensional thickness of sediments $h\sigma/D$ in a sedimentary basin as a function of nondimensional time $t\sigma^2/D$ for a sequence in which the ratio of the standard deviation to the mean of sedimentation, $\sigma/\tilde{\eta}$ is 0.1. **B)** For the model given in A, the age of the sediments as a function of depth. Only those sediments which are not later eroded are preserved.

representing subsidence of the basin at a constant rate. The time series is scale invariant in terms of the nondimensional sedimentary thickness $h\sigma/D$ and time $t\sigma^2/D$; it is characterized by the single parameter $\sigma/\bar{\eta}$. If $\sigma/\bar{\eta}$ is small the fluctuations in sedimentation rate are small compared to the subsidence rate; if $\sigma/\bar{\eta}$ is large the fluctuations are large. For the example given in Figure 2A, $\sigma/\bar{\eta} = 0.1$. Figure 2B is produced from Figure 2A by removing any deposited sediment that is subsequently eroded. In the "staircase" plot of Figure 2B, beds are defined as a time interval of continuous deposition, i.e., a series of consecutive timesteps with different elevations. Hiatuses are defined as periods in which no sediment is preserved, i.e., a series of consecutive timesteps with the same elevation.

We will next discuss the relationship between sedimentation rate and time span with the stratigraphic model of Plotnick (1986) based on a deterministic fractal distribution of hiatus lengths. The age of sediments in this model is given as a function of depth in Figure 3A. As illustrated, the vertical segments (beds) are of equal thickness. The positions of the transitions from beds to hiatuses are given by a second-order Cantor set. Eight kilometers of sediments have been deposited in this model sedimentary basin in a period of 9 Myr so that the mean rate of deposition is R (9 Myr) = 8 km/9 Myr = 0.89 mm/yr over this period. However, there is a major
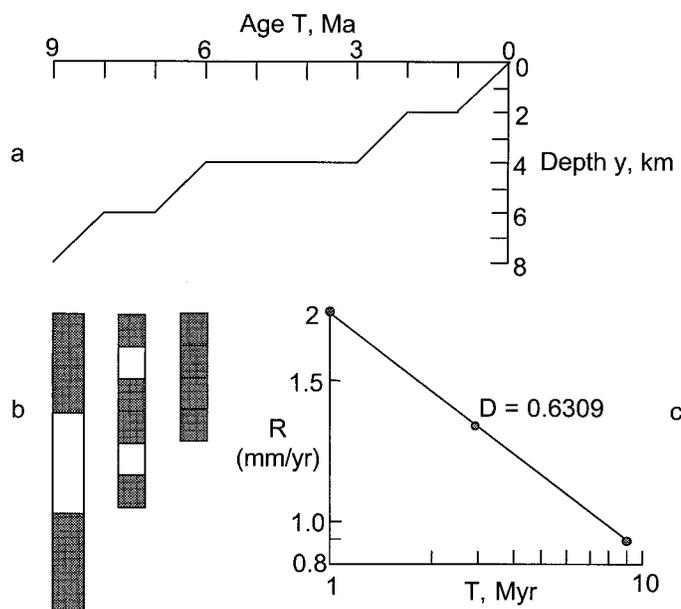
FIG. 3.—Illustration of a model for sediment deposition based on a Devil's staircase associated with a second-order Cantor set. **A)** Age of sediments T as a function of depth y. **B)** Illustration of how the Cantor set is used to construct the sedimentary pile. **C)** Average rate of deposition R as a function of the period T considered.

FIG. 4.—Average rate of sedimentation, $R/\bar{\eta}$, as as a function of time span, $T\sigma^2/D$, for the sediment column of Figure 2B.

unconformity at a depth of 4 km. The sediments immediately above this unconformity have an age of 3 Ma and the sediments immediately below it have an age of 6 Ma. There are no sediments in the sedimentary pile with ages between 3 and 6 Ma. In terms of the Cantor set this is illustrated in Figure 3B. The line of unit length is divided into three parts and the middle third, representing the period without deposition, is removed. The two remaining parts are placed on top of each other as shown.

During the first three million years of deposition (the lower half of the sedimentary section) the mean rates of deposition are R (3 Myr) = 4 km/3 Myr = 1.33 mm/yr. Thus the rate of deposition increases as the period considered decreases. This is shown in Figure 3C.

There is also an unconformity at a depth of two kilometers. The sediments immediately above this unconformity have an age of 1 Ma and sediments below have an age of 2 Ma. Similarly there is an unconformity at a depth of 6 km; the sediments above this unconformity have an age of 7 Ma and sediments below an age of 8 Ma. There are no sediments in the pile with ages between 7 and 6 Ma or between 2 and 1 Ma. This is clearly illustrated in Figure 3A. In terms of the Cantor set (Fig. 3B), the two remaining line segments of length ⅓ are each divided into three parts and the middle thirds are removed. The four remaining segments of length ⅑ are placed on top of each other as shown. During the periods 9 to 8, 7 to 6, 3 to 2, and 1 to 0 Ma the rates of deposition are R (1 Myr) = 2 km/1 Myr = 2 mm/yr. This rate is also included in Figure 3C.

The rate of deposition clearly has a power-law dependence of the length of the time interval considered. The results illustrated in Figure 3 are based on a second-order Cantor set, but the construction can be extended to any order desired and the power-law results given in Figure 3C would be extended to shorter and shorter time intervals.

The sedimentation rate has been calculated in this way based on the sedimentation history of Figure 2. The results are plotted in Figure 4 on a logarithmic scale. The sedimentation rate has a power-law dependence on time span with exponent $-\tfrac{3}{4}$: $R \propto T^{-\tfrac{3}{4}}$. Sadler and Strauss have shown that the random-walk model results in a power-law relationship with exponent $-\tfrac{1}{2}$. The dependence of sedimentation rate on time span predicted by our model is a better fit to the data of Sadler (1981) than that of the
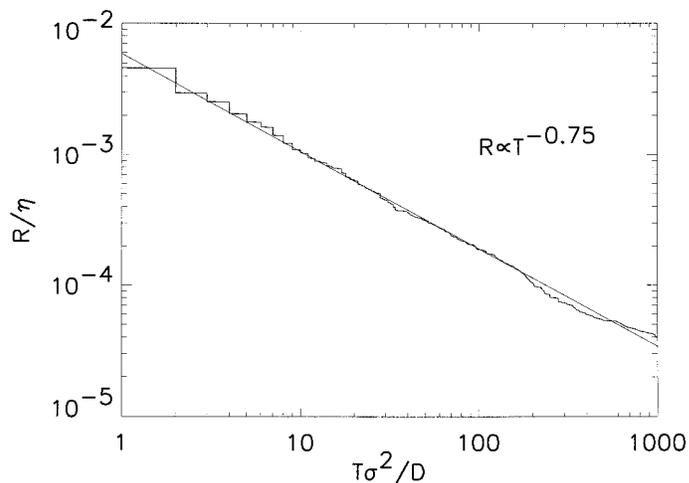
random-walk model. Sadler (1981) has compiled measurements of fluvial sedimentation rates from the geological literature from time scales of minutes to 100 million years. His data (Sadler 1995) are plotted in Figure 5, where they are averaged in bin sizes logarithmically increasing in time. In this plot we have not included the data on time scales from 10^5 to 10^8 years because these time scales include unconformities resulting from regressive and transgressive events on active continental margins. Variations in sea level are beyond the scope of the model, and it would be inappropriate to compare the model to sedimentation rates on those time scales. A least-squares linear fit to the logarithms (base 10) of the data yields a slope of -0.76. This result is consistent with the analysis of the model given in Figure 4.

These results can also be obtained from theoretical fractal relations. Fractional Brownian walks have the property that the standard deviation of the time series has a power-law dependence on time with a fractional exponent called the Hausdorff measure, Ha: $\sigma \propto T^{Ha}$. The rate of change of the time series for a given time interval, T, is then the sedimentation rate $R = \sigma/t \propto T^{Ha-1}$. The power spectral exponent of a time series and its Hausdorff measure have been related theoretically by $\beta = 2Ha + 1$ (Turcotte 1992).
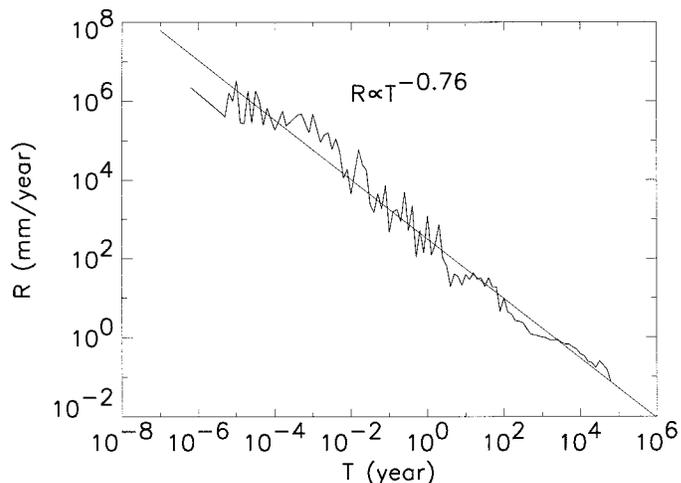

FIG. 5.—Observed sedimentation rates as a function of time span, from Sadler (1981). The data have been binned logarithmically to obtain a uniform distribution of points in log-log space. A least-squares linear fit to the logarithms of the data yields a slope of $-\tfrac{3}{4}$, indicating that $R \propto T^{-\tfrac{3}{4}}$.
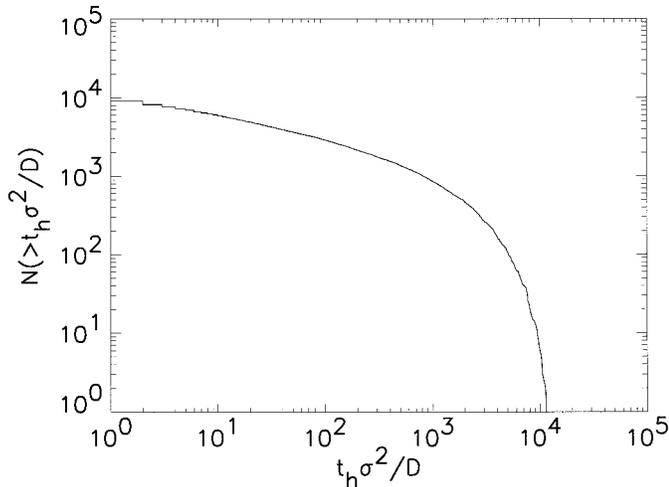
FIG. 6.—Cumulative frequency-length distribution of hiatuses, the number of hiatuses longer than nondimensional hiatus length $t\,\sigma^2/D$, for synthetic sequences produced with the stochastic diffusion model.

FIG. 7.—Cumulative frequency-thickness distribution of nondimensional bed thicknesses for synthetic sediment columns with $\sigma/\bar{\eta} = 0.1$, 0.01, 0.001, and 0.0003. The graph scales are log-linear. The distributions are exponential.

For the random-walk model, $\beta = 2$, $Ha = \frac{1}{2}$, and the sedimentation rate is then $R \propto T^{-\frac{1}{2}}$. For the stochastic diffusion model, $\beta = 3/2$, $Ha = \frac{1}{4}$, and $R \propto T^{-\frac{3}{4}}$, in agreement with the numerical results.

The dependence of sedimentation rate on time span continues up to time scales of the Wilson cycle. On time scales of 10^5–10^8 years transgressive and regressive events give rise to alternating periods of deposition and erosion as mentioned previously. Korvin (1992) found, using the SEDPAK simulation package, that alternating periods of deposition and erosion resulting from sea-level change, combined with the diffusive parameterization of sediment transport of SEDPAK, resulted in a decreasing sedimentation rate with increasing time span in the same way that channel avulsion and diffusive sediment transport results in episodic sedimentation rates on smaller time scales.

DISTRIBUTIONS OF BED THICKNESS AND HIATUS LENGTH

Working from our preserved thickness history of Figure 2B, we will define a bed as any consecutive sequence of time units with different thickness. Conversely, a hiatus is any consecutive sequence of time units with the same thickness. In this section we will present distributions of bed thickness and hiatus length and compare them with observations and with other models.

Plotnick (1986) presented the model for discontinuous sedimentation based on a fractal distribution of hiatus lengths presented in Figure 3. The cumulative distribution of hiatus lengths, the number of hiatuses greater than or equal to a length of time, T, produced by our model is plotted in Figure 6. In order to obtain an accurate curve, we generated 100 synthetic preserved thickness histories and accumulated the hiatus distributions to obtain Figure 6. The distribution is not fractal. This was at first surprising because a fractal distribution of hiatuses was used to illustrate how a power-law dependence of sedimentation rate on time span can occur. However, in the model of Figure 3 each bed had the same thickness. In contrast, as we will show, the stochastic diffusion model of sedimentation results in bed thicknesses with an exponential distribution. Therefore, our observation of a scale-invariant sedimentation rate without a scale-invariant distribution of hiatuses is not inconsistent with the model of Figure 3 because they result in different bed-thickness distributions.

The cumulative distribution of bed thicknesses generated by our model is plotted in Figure 7 for the four different values of $\sigma/\bar{\eta}$ indicated next to each distribution. Note that the graph scales are log-linear. For synthetic depositional histories with a relatively large $\s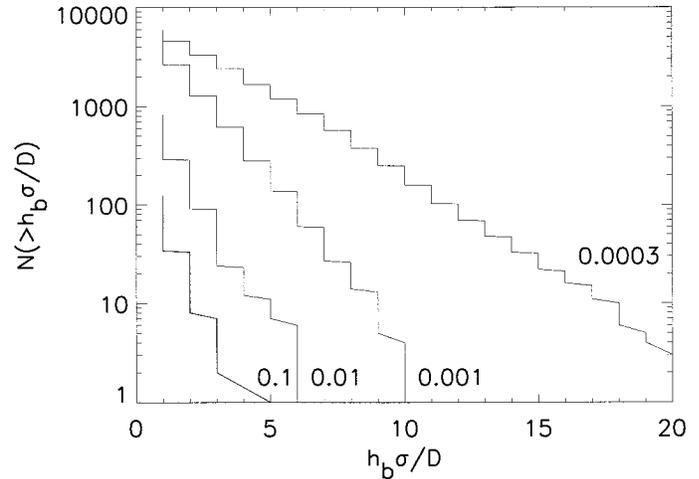igma/\bar{\eta}$, such as 0.1, no deposition occurs during most of the history. The result is a small number of beds with a very skewed distribution. For smaller ratios, more thick beds appear in the record. The straight-line trends of the distributions on a log-linear axis indicate that the cumulative bed-thickness distributions are exponential. The probability density function is also exponential because the cumulative distribution is the integral of the probability density function. Exponential bed-thickness distributions are common in stochastic models of sedimentation (Dacey 1979). Despite reported conclusions that stochastic models of sedimentation, including those that generate exponential bed-thickness distributions, accurately predict observed bed-thickness distributions (Mizutani and Hattori 1972), we are not aware of any model that predicts the commonly observed lognormal distribution. This may be a fundamental weakness of the bed-formation models that have been proposed to date. Another possibility has been suggested by Drummond and Wilkinson (1996). They argued that the observation of lognormal distributions is an artifact resulting from unrecognized or unrecorded thin strata. They propose that exponential distributions are consistent with the data if the data for the frequencies of the smallest strata are considered incomplete and not considered in the distribution fitting. This is consistent with the conclusion of Muto (1995), who presented the cumulative frequency-thickness distribution of four large turbidite datasets from Japan. He found that an exponential distribution best fits the data. However, power-law distributions have also been persuasively argued for the distribution of turbidites (Rothman et al. 1993).

In Figure 7, synthetic sedimentation histories with larger values of sedimentation rate, $\sigma/\bar{\eta}$, have a more skewed distribution or a steeper slope on a log-linear scale. This is consistent with the dependence of skew on sedimentation rate that can be observed in deep-sea sequences presented in Claps and Masetti (1994). Until now we have applied our model only to fluvial depositional environments, where the association of the diffusion and random terms with basic geomorphologic concepts (sediment transport by overland and channel flow and channel avulsion, respectively) is most easily accomplished. However, the universal dependence of sedimentation rate on time span for the different environments analyzed by Sadler (1981) and for deep-sea sequences by Moore and Heath (1977) suggests basic similarity in the dynamics of sedimentation despite certain differences. If deep-sea sedimentation by turbidites contains spatial and temporal variability in transport and lateral spreading of the deposited sediment, a stochastic diffusion model may be applicable to describing some of the dynamics of deep-sea sequences. Claps and Masetti (1994) published bed-thickness data from three formations in Italy: Ra Stua, Castagne, and Cis-
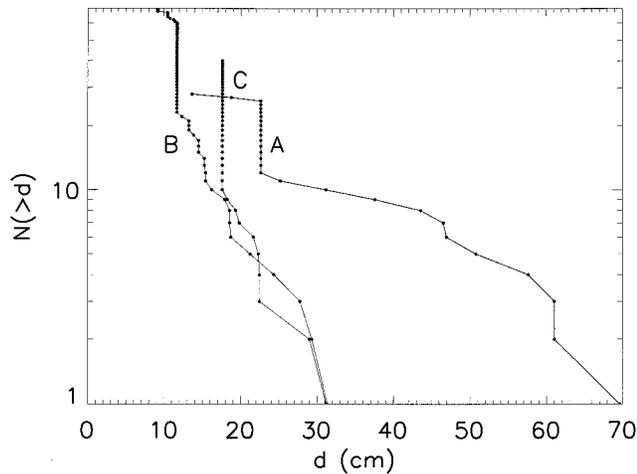
FIG. 8.—Cumulative frequency-thickness distribution of bed thicknesses of deep-sea sequences from **A)** Ra Stua, **B)** Castagne, and **C)** Cismon Valley, Italy published by Claps and Masetti (1994). The coefficients in the exponential distributions determined by a least-squares fit of the logarithm of the bed number to the bed thickness for the largest forty beds were -0.052, -0.166, and -0.252, showing an increasing trend with sedimentation rate consistent with the model behavior.

mon Valley. The sedimentation rates for a 1 Ma time scale have been estimated to be 2.5, 1.7, and 0.6 cm/ka, respectively, for these sections. In Figure 7 we found that basins which filled slowly had bed-thickness distributions that were more skewed than those in basins which filled more quickly. This is consistent with the observed dependence of skew on sedimentation rate for the three sequences, as shown in Figure 8. The cumulative bed-thickness distributions for these sections based on data that were digitally scanned from Claps and Masetti (1994) are presented in Figure 8. The model prediction that the skew of the bed-thickness distributions increases from the (A) Ra Stua section to the (B) Castagne and (C) Cismon Valley sections is consistent with the data.

PERSISTENCE AND CYCLICITY IN BED THICKNESS SEQUENCES

Many workers have performed time-series analysis of bed-thickness sequences as a function of depth to identify periodic forcings such as Milankovitch cycles (DeBoer and Smith 1994). However, some doubt whether a periodic forcing would manifest itself simply and linearly as a periodicity in a bed-thickness sequence, as is often assumed given the complexity of basin response to climate or sea-level variations (Herbert 1994; Smith 1994). We have performed simple numerical experiments to address this question.

As a control, we have performed spectral analysis on the time series of bed thicknesses as a function of depth generated by the stochastic diffusion model. This model can be considered to be a null model representing autocyclic processes often present in a fluvial sedimentary system.

We have performed spectral analyses of the bed-thickness series generated by our model for different values of $\sigma/\bar{\eta}$. We used power spectral analysis to quantify the persistence. For each ratio, we generated one hundred synthetic depositional histories, extracted the bed-thickness series for each history, computed the power spectrum, and averaged the power spectra at equal frequency values. Since the bed thicknesses as a function of depth result in a series that is nonuniformly spaced as a function of depth, conventional techniques of power spectral estimation using the Fast Fourier Transform (FFT) cannot be used. Instead, we used the Lomb Periodogram, suggested by Press et al. (1992) for power spectral estimation with nonuniformly sampled data. We found no evidence for persistence in any of the synthetic bed-thickness series. The power spectra were white, indicating that bed thicknesses in the model are independent of one another. This
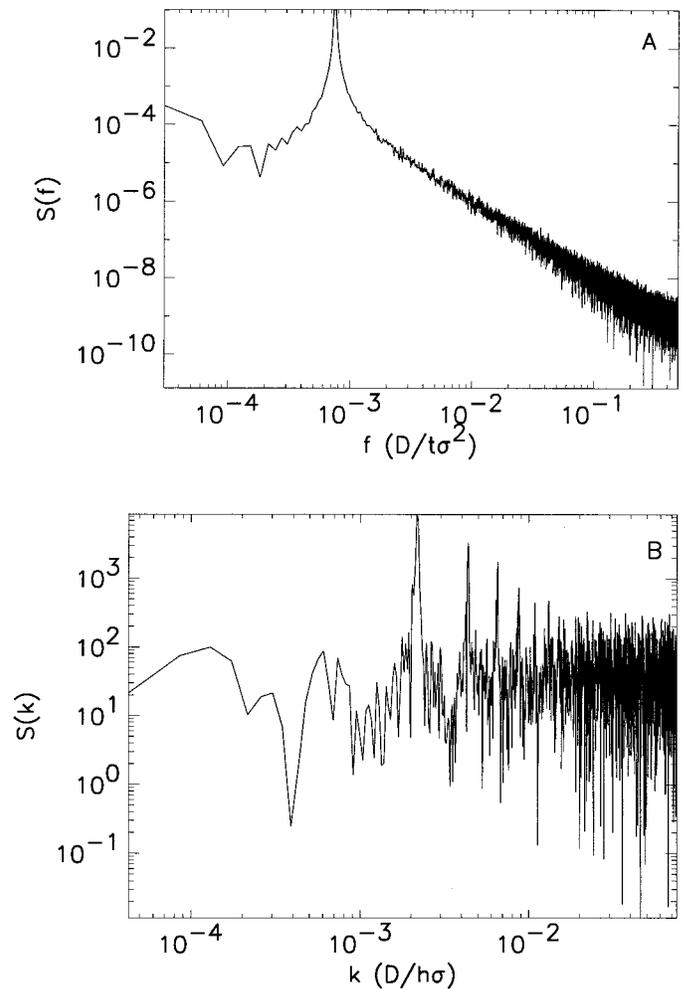

FIG. 9.—**A)** Power spectrum of synthetic history of deposition and erosion with a strong periodocity superimposed on the model behavior with $S(f) \propto f^{-3/2}$. **B)** Power spectrum of series of bed thickness as a function of depth showing periodic behavior associated with the periodic forcing in the sedimentation process.

result is counterintuitive because episodes of deposition and erosion are not independent, as in a random-walk model, and we expected this anti-correlation to be reflected in some persistence in the synthetic bed-thickness sequences. If the model presented in this paper fully characterizes the essential dynamics of autocyclic processes in fluvial sedimentary basins, then the lack of persistence that we observe in the synthetic sequences suggests that any persistence or cyclic behavior must be the result of allocyclic processes such as climatic or tectonic forcing.

We also considered the persistence and distribution of bed thicknesses with a periodic forcing superimposed on the stochastic diffusion model. For this synthetic history of deposition and erosion we synthesized a time series with the model power spectrum of $S(f) \propto f^{-3/2}$ as before. We then chose an intermediate frequency and multiplied the Fourier coefficients at that frequency by a factor of 1000. The power spectrum of the synthetic depositional and erosional history created this way is presented in Figure 9A. The power spectrum of the series of bed thicknesses as a function of depth, estimated using the Lomb Periodogram, is presented in Figure 9B. The periodic component is found to be preserved in the record. This result suggests that it is possible to identify periodic forcings in the stratigraphic record despite the superposition of autocyclic and allocyclic processes in the history of deposition and erosion. However, it should be noted that the amplitude of the periodic signal has been significantly reduced in the syn-
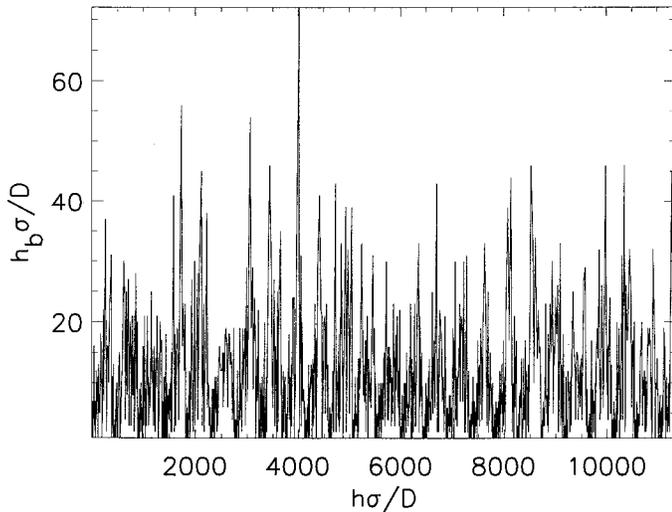
thetic stratigraphy. Power has also been introduced at higher harmonics of the forcing frequency, further complicating the spectrum of the stratigraphic response.

The sequence of beds as a function of depth in the synthetic history of Figure 9 is shown in Figure 10. This series shows that although there is a strong periodicity in the history of deposition and erosion, a broad distribution of bed thicknesses results. Some studies have presented unimodal bed-thickness distributions from fluvial sedimentary environments as evidence for periodic forcing in the stratigraphic record (e.g., Olsen 1994). Figure 10 implies that as long as there are variations in the depositional and erosional history at frequencies higher than the external forcing frequency, any uniformly thick beds that would have been formed corresponding to the periodicity of the forcing frequency have been broken up by the higher-frequency variations. In fact, the distribution of bed thicknesses of the sequence from Figure 10 is indistinguishable from the exponential distribution observed in synthetic bed sequences with no periodic forcing. It can be concluded from this that periodicities in the sedimentation history need not result in a unimodal bed-thickness distribution. This has also been argued with numerical experiments by Goldhammer et al. (1990). It also suggests that no matter what periodic forcings are present, unimodal distributions should not be expected if the stochastic diffusion model applies to the dynamics of the basin. The model may not be applicable to a basin in which channel avulsion is rare, for instance. Another possible reason for the observation of unimodal bed thicknesses is that the true distribution is exponential but many thin beds are unrecognized (Drummond and Wilkinson 1996).

CONCLUSIONS

We investigated the synthetic stratigraphy of a model of fluvial sedimentation that extends the classic random-walk model to include sediment transport modeled by the diffusion equation (Culling's model). The model is found to have a sedimentation rate that depends on time scale as a power law with exponent $-\frac{3}{4}$, in excellent agreement with the observations of Sadler (1981). The model may be useful as a null model representing autocyclic or internal dynamics of a fluvial sedimentary basin. The effects of hypothesized allocyclic processes can be superimposed on the dynamics of this model as part of a forward modeling study of the stratigraphic response expected from the allocyclic behavior. As an example of this, we consider the effects of a periodic external forcing superimposed on the stochastic diffusion model. The results suggest that any persistence observed in bed-

thickness sequences by time-series analysis is the result of external (climatic or tectonic) forcing and that care should be taken in interpreting unimodal bed-thickness distributions as the result of periodic forcing.

REFERENCES

BEERBOWER, J.R., 1964, Cyclothems and cyclic depositional mechanisms in alluvial plain sedimentation: Kansas Geological Survey, Bulletin 169, p. 31–42.
BEGIN, Z.B., MEYER, D.F., AND SCHUMM, S.A., 1981, Development of longitudinal profiles of alluvial channels in response to base level lowering: Earth Surface Processes, v. 6, p. 49–68.
BRIDGE, J.S., AND LEEDER, M.R., 1979, A simulation model of alluvial stratigraphy: Sedimentology, v. 26, p. 617–644.
CLAPS, M., AND MASETTI, D., 1994, Milankovitch periodicities recorded in Cretaceous sequences from the Southern Alps (Northern Italy), *in* De Boer, P.L., and Smith, D.L., eds., Orbital Forcing and Cyclic Sequences: Cambridge, Massachusetts, Blackwell, p. 99–107.
CULLING, W.E.H., 1965, Theory of erosion of soil-covered slopes: Journal of Geology, v. 73, p. 230–254.
DACEY, M.F., 1979, Models of bed formation: Mathematical Geology, v. 11, p. 655–668.
DE BOER, P.L., AND SMITH, D.G., 1994, Orbital forcing and cyclic sequences, *in* De Boer, P.L., and Smith, D.L., eds., Orbital Forcing and Cyclic Sequences: Cambridge, Massachusetts, Blackwell, p. 1–14.
DRUMMOND, C.N., AND WILKINSON, B.H., 1996, Stratal thickness frequencies and the prevalence of orderedness in stratigraphic sequences: Journal of Geology, v. 104, p. 1–18.
DUNNE, T., WHIPPLE, K.X., AND AUBRY, B.F., 1995, Microtopography of hillslopes and initiation of channels by Horton overland flow: Geophysical Monographs, v. 89, p. 27–44.
EDWARDS, S.F., AND WILKINSON, D.R., 1982, The surface statistics of a granular aggregate: Royal Society [London], Proceedings, ser. A, v. 381, p. 17–31.
FAMILY, F., 1986, Scaling of rough surfaces: effects of surface diffusion: Journal of Physics A, v. 19, p. L441–L446.
GILL, M.A., 1983a, Diffusion model for aggrading channels: Journal of Hydraulic Research, v. 21, p. 355–367.
GILL, M.A., 1983b, Diffusion model for degrading channels: Journal of Hydraulic Research, v. 21, p. 369–378.
GOLDHAMMER, R.K., DUNN, P.A., AND HARDIE, L.A., 1990, Depositional cycles, composite sea level changes, cycle stacking patterns, and the hierarchy of stratigraphic forcing: Examples from Alpine Triassic platform carbonates: Geological Society of America, Bulletin, v. 102, p. 535–562.
GUCCIONE, M.J., 1993, Grain-size distribution of overbank sediment and its use to locate channel positions, *in* Marzo, M., and Arergas, C.P., eds., Alluvial Sedimentation: Cambridge, Massachusetts, Blackwell, p. 185–194.
HANKS, T.C., BUCKMAN, R.C., LAJOIE, K.R., AND WALLACE, R.E., 1984, Modification of wave cut and faulting-controlled landforms: Journal of Geophysical Research, v. 89, p. 5771–5790.
HANKS, T.C., AND WALLACE, R.E., 1985, Morphological analysis of the Lake Lahontan shoreline and beachfront fault scarps, Pushing County, Nevada: Seismological Society of America, Bulletin, v. 75, p. 835–846.
HERBERT, T.D., 1994, Reading orbital signals distorted by sedimentation: Models and examples, *in* De Boer, P.L., and Smith, D.L., eds., Orbital Forcing and Cyclic Sequences: Cambridge, Massachusetts, Blackwell, p. 483–507.
HEWETT, T.A., 1986, Fractal distribution of reservoir heterogeneity and their influence of fluid transport: Society of Petroleum Engineers, 61st Annual Technical Conference, New Orleans.
HOLLIGER, K., 1996, Upper-crustal seismic velocity heterogeneity as derived from a variety of P-wave sonic logs: Geophysical Journal International, v. 125, p. 813–829.
KENYON, P.M., AND TURCOTTE, D.L., 1985, Morphology of a delta prograding by bulk sediment transport: Geological Society of America, Bulletin, v. 96, p. 1457–1465.
KOLMOGOROV, A.N., 1951, Solution of a problem in probability theory connected with the problem of the mechanism of stratification: American Mathematical Society, Transactions, v. 53, p. 171–177.
KORVIN, G., 1992, Fractal Models in the Earth Sciences: Amsterdam, Elsevier, 396 p.
MACKEY, S.D., AND BRIDGE, J.S., 1995, Three-dimensional model of alluvial stratigraphy: theory and application: Journal of Sedimentary Research, v. B65, p. 7–31.
MIZUTANI, S., AND HATTORI, I., 1972, Stochastic analysis of bed-thickness distribution of sediments: Mathematical Geology, v. 4, p. 123–146.
MOORE, T.C., AND HEATH, G.R., 1977, Survival of deep-sea sedimentary sections: Earth and Planetary Science Letters, v. 37, p. 71–80.
MUTO, T., 1995, The Kolmogorov model of bed thickness distribution: An assessment based on numerical simulation and field-data analysis: Terra Nova, v. 7, p. 408–416.
NASH, D., 1980, Forms of bluffs degraded for different lengths of time in Emmet County, Michigan, USA: Earth Surface Processes, v. 5, p. 331–345.
OLSEN, H., 1994, Orbital forcing on continental depositional systems—lacustrine and fluvial cyclicity in the Devonian of East Greenland, *in* De Boer, P.L., and Smith, D.L., eds., Orbital Forcing and Cyclic Sequences: Cambridge, Massachusetts, Blackwell, p. 429–438.
PELLETIER, J.D., AND TURCOTTE, D.L., 1996, Scale-invariant topography and porosity variations in fluvial sedimentary basins: Journal of Geophysical Research, v. 101, p. 28,165–28,175.

PILKINGTON, M., AND TODOESCHUCK, J.P., 1990, Stochastic inversion for scaling geology: Geophysical Journal International, v. 102, p. 205–217.

PIZZUTO, J.E., 1987, Sediment diffusion during overbank flows: Sedimentology, v. 34, p. 301–317.

PLOTNICK, R.E., 1986, A fractal model for the distribution of stratigraphic hiatuses: Journal of Geology, v. 94, p. 885–890.

PRESS, W.H., TEUKOLSKY, S.A., VETTERLING, W.T., AND FLANNERY, B.P., 1992, Numerical Recipes in C: The Art of Scientific Computing, 2nd Edition: New York, Cambridge University Press, 994 p.

ROTHMAN, D.H., GROTZINGER, J.P., AND FLEMINGS, P.B., 1993, Scaling in turbidite deposition: Journal of Sedimentary Petrology, v. A64, p. 59–67.

SADLER, P.M., 1981, Sediment accumulation rates and the completeness of stratigraphic sections: Journal of Geology, v. 89, p. 569–584.

SADLER, P.M., AND STRAUSS, D.J., 1990, Estimation of completeness of stratigraphical sections using empirical data and theoretical methods: Geological Society of London, Journal, v. 147, p. 471–485.

SCHWARZACHER, W., 1975, Sedimentation Models and Quantitative Stratigraphy: Amsterdam, Elsevier, 382 p.

SMITH, D.G., 1994, Cyclicity or chaos? Orbital forcing versus non-linear dynamics, *in* De Boer, P.L., and Smith, D.L., eds., Orbital Forcing and Cyclic Sequences: Cambridge, Massachusetts, Blackwell, p. 531–544.

STRAUSS, D.J., AND SADLER, P.M., 1989, Stochastic models for the completeness of stratigraphic sections: Mathematical Geology, v. 21, p. 37–59.

TIPPER, J.C., 1983, Rates of sedimentation and stratigraphical completeness: Nature, v. 21, p. 296–298.

TODOESCHUCK, J.P., JENSEN, O.G., AND LABONTE, S., 1990, Gaussian scaling noise model of seismic reflection sequences: Evidence from well logs: Geophysics, v. 55, p. 480–484.

TUBMAN, K.M., AND CRANE, S.D., 1995, Vertical versus horizontal well log variability and application to fractal reservoir modeling, *in* Barton, C.C., and LaPointe, P.R., eds., Fractals in Petroleum Geology and Earth Sciences: New York, Plenum, p. 279–294.

TURCOTTE, D.L., 1992, Fractals and Chaos in Geology and Geophysics: New York, Cambridge University Press, 221 p.

WALDEN, A.T., AND HOSKEN, J.W.J., 1985, An investigation of the spectral properties of primary reflection coefficients: Geophysical Prospecting, v. 33, p. 400–435.

WALLACE, R.E., 1977, Profiles and ages of young fault scarps, north-central Nevada: Geological Society of America, Bulletin, v. 88, p. 1267–1281.